JOURNAL OF MATERIALS SCIENCE 37 (2002) 4717–4731

Development and measurement of stress in polymer coatings

L. F. FRANCIS*, A. V. McCORMICK, D. M. VAESSEN
Department of Chemical Engineering and Materials Science, University of Minnesota, Minneapolis, MN 55455, USA
E-mail: lfrancis@tc.umn.edu

J. A. PAYNE
Eastman Kodak Company, Rochester, NY 14652, USA

This paper reviews stress development mechanisms and stress measurement techniques for polymer coatings. Most polymeric coatings shrink during and after solidification due to chemical reaction, solvent evaporation, phase separation, or some combination thereof. Coating adhesion, however, prevents shrinkage from occurring freely; this frustration of in-plane shrinkage leads to a tensile stress in the plane of the coating. At the same time, stress accumulates, it may be relaxed by processes such as molecular motion. The measured stress at any time is the result of the competition between stress buildup from frustrated shrinkage and stress relief from relaxation. Accumulation of stress is a problem because it can lead to defects such as cracks. An understanding of stress development in various types of polymeric coating systems will lead to strategies for material selection, process optimization, and defect elimination. In this paper, background on stress development is provided, followed by an overview of stress measurement methods for polymer coatings. The remainder of the paper focuses on stress development during the drying and curing of polymer coatings, drawing many examples from previous stress measurement studies.

1. Introduction

Polymer coatings inherently develop stress during processing. Polymer coatings are prepared by depositing a liquid onto a substrate and converting the as-deposited liquid layer into a solid. The liquid can be a polymer dissolved in a solvent, a monomer or an oligomer with an initiator, or a suspension of polymer latex particles. Solidification of the as-deposited liquid layer into a solid coating is typically driven by solvent removal (i.e., gelation, vitrification, crystallization, or coalescence on drying) or reaction (i.e., polymerization on thermal or radiation curing). Regardless of the solidification process, the coating undergoes a major change in structure and properties during solidification. Solidification is ordinarily accompanied by shrinkage. After the coating has developed enough elasticity to support a stress, shrinkage in the plane of the coating is constrained by adhesion to the substrate, and hence an in-plane tensile stress develops. As described more completely below, this shrinkage coupled with the evolving coating properties determines how stress develops during processing and the 'final' stress in the coating after processing is complete.

Temperature plays a key role in solidification and coating stress development. Increasing the temperature, raises the drying and reaction rates, on which stress usually scales. However, for a polymer coating of given solvent content or extent of reaction, stresses relax more quickly as temperature is raised [1]. Decoupling these two effects is challenging. Temperature changes also drive solidification for some coatings; for example, the gelatin layer in photographic film is solidified by chilling before it is dried [2], and thermoplastic powder coatings become solid on cooling. Coating stress is also affected by the temperature change itself due to thermal expansion mismatch with the substrate [3, 4]. This 'thermal stress' is sometimes distinguished from 'intrinsic stress' or 'growth stress', which is ascribed to the stresses developing during the formation of the coating itself, and 'external stress', which is applied mechanically [3].

Stress development from constrained shrinkage and volume changes is not unique to polymer coatings. Ceramic and metal coatings and thin films prepared by sputtering, chemical vapor deposition, and other vapor-phase routes also develop stresses during their growth [3–7]. Multilayer assemblies and other composite structures develop stress [8–10]. In fact, most systems in which two dissimilar solids are joined are likely to develop stresses from temperature excursions and during processing.

Stress itself is not typically a concern, except when the stresses induce defects [11, 12]. When a coating on a flexible substrate develops stress, the substrate

*Author to whom all correspondence should be addressed.

deforms in response to stress, a phenomenon known as 'curling' [11, 13]. If a brittle coating is under stress and the stress exceeds the coating strength, cracks will form [14–19]. If the interface between coating and substrate is weak enough, coating stress leads to delamination, (i.e., cracking at the interface) [17, 20–22]. Stresses are also magnified near particle inclusions [19, 23], causing additional local defects.

Stresses in coatings can impact their properties and those of the underlying material. Stresses in coatings on optical fibers can lead to bending and therefore, transmission loss [24]. The patterning resolution of some photoresists is reduced by differences in stress between exposed and unexposed areas of the coating [25]. Stress in the gelatin-based imaging layers leads to degradation in image quality [26]. Stress in a coating designed for corrosion protection may limit its ability to protect the underlying substrate from corrosive attack [27–29]. Likewise, stresses in protective coatings on artwork can limit their performance [30].

Over time and during use, the stress in a coating may change. Weathering from exposure to different temperatures, sunlight, and relative humidity changes the coating's chemical structure and composition, and may alter the coating stress, as recently reviewed by Perera [29]. Tensile stresses developed during coating processing may increase or decrease with time, depending on the environmental conditions and the coating chemistry. Conditions of high relative humidity tend to decrease tensile stress and even lead to compressive stresses as moisture is absorbed into a coating.

Stress in polymer coatings has been studied for many years. Coating engineers and researchers have been concerned with measuring and understanding the origin of stress, as well as finding ways to avoid stress and its effects. Reports of stress measurement in polymer coatings began to appear with frequency in the late 1970s and 1980s. Croll [20, 31–37] and Perera and coworkers [38–45] were among the most productive and influential in establishing the measurement methods and the basis for understanding the origin of stress. In recent years, interest in stress development in polymer coatings continues to grow. New coating systems involving ultraviolet (UV) and electron beam radiation curing have come into prominence in the wake of environmental concerns over volatile organic compounds. Polymer and organic-inorganic hybrid coatings continue to be developed for applications in microelectronics and related fields. Moreover, measurements of stress can reveal information about the microstructure and properties of coatings.

This paper reviews the stress development in polymer coatings, drawing examples from some recent stress measurement studies. The next section presents some background on stress development followed by a synopsis of stress measurement methods for polymer coatings. Stress measurement results and analyses are then presented for two classes of coatings: those that solidify by drying and those that solidify by curing. We attempt to provide an overview and a good representation of research underway in this large field. However, the scope of the paper is limited and some topics, such as latex-based coatings and powder coatings, are not included.

2. Background on stress development

The principles of stress development in polymer coatings are most easily introduced by considering first the shrinkage of a solid, elastic coating anchored to a rigid substrate. This problem has been considered in the analysis of stresses caused by thermal expansion mismatch [4, 6, 46] and other situations involving constrained volume change. Croll's [31–33] research on the origin of stress in polymer coatings also takes this approach. The background laid out below is based on these past researches as well as the work carried out by Scriven [47], Tam [48, 49], Lei [18, 23, 50] and Wen [51, 52]. The discussion below is largely qualitative with some illustrations from the theoretical work of Lei [18, 50]. Readers interested in a more rigorous, quantitative treatment of stress development in polymer coatings should consult the references given above.

In the simplest case, stress in a polymer coating begins to develop when the coating has dried or cured enough so that it has developed elasticity and can support a stress. Croll [31] defined this initial "solidified" state in drying polymer solution coatings as the point at which the glass transition temperature of the coating (which is a function of solvent content) is equal to the drying temperature. Further shrinkage from this initial state occurs freely in the thickness direction, but is constrained in the plane of the coating. As shrinkage proceeds, the current state of the coating departs from its stress-free state [18, 47, 49], as illustrated in Fig. 1a. This departure results in a strain. The stress-free state can be thought of as the state that the coating would adopt if it were removed from the substrate. Like the current state, the stress-free state changes during drying or curing. The in-plane stress in the coating at a time t, $\sigma(t)$, is product of the strain at that time, $\varepsilon(t)$ (i.e., the difference between the current state and the stress-free state) and the elastic properties of the coating:

$$\sigma(t) = \frac{E_c}{1 - \nu_c}\varepsilon(t), \tag{1}$$

where E_c is the elastic modulus of the coating, and ν_c is the Poisson's ratio of the coating.

Away from the edge of the coating, the stress due to constrained shrinkage is tensile and in the plane of the coating [4, 21, 49, 53]. Hence, the biaxial modulus ($E_c/(1 - \nu_c)$) in Equation 1 is appropriate. Near the edge, shear and out-of-plane (i.e., peeling) stresses appear, but these decay to zero at a distances of a few coating thicknesses from the edge [4, 21, 49, 53]. The state of stress near edges and other discontinuities such as particles [18, 19, 23] is of particular importance to the understanding of how stress-induced defects arise.

As shrinkage continues, strain climbs and so does the stress. Equation 1 assumes that an elastic modulus appears when the coating has solidified and that it remains constant [31], However, the elastic modulus will continue to grow as solvent is removed by drying or

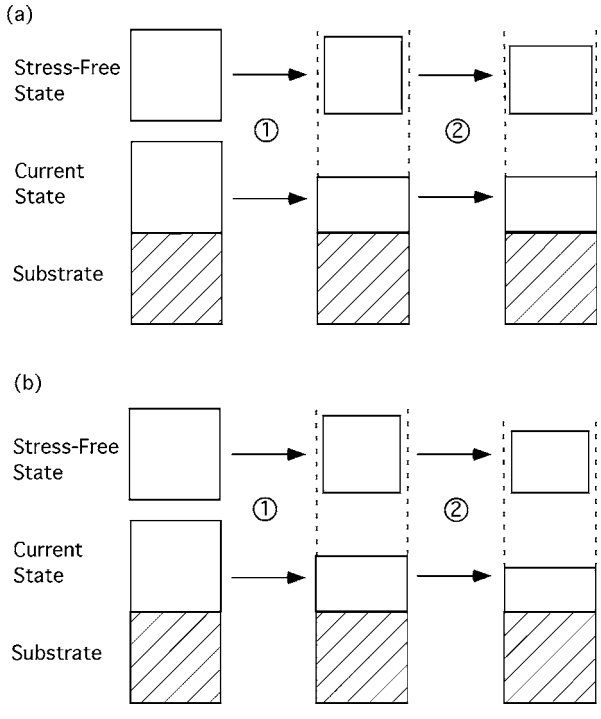

Figure 1 Strain development in a segment of the coating far from the edge. (a) A viscoelastic coating. At solidification (left), the current state and stress-free state are indentical. During shrinkage in step 1, the stress-free state shrinks isotropically and the current state shrinks only out of plane. In step 2, stress relaxation takes place with no shrinkage; the stress-free state expands and the strain is reduced. An elastic coating undergoes step 1 only. (b) An elastic-plastic coating. The total deformation is the summation of an elastic deformation in step 1 (as above) and a plastic deformation in step 2 in which shrinkage continues but the stress-free state does not deform in the plane of the coating and hence strain remains constant. Adapted from Scriven [47], Tam [49], and Lei [18, 50].

as more crosslinks are established by curing reactions. Hence, E_c and to a lesser extent ν_c vary with time and the magnitude of the coating stress at any point after solidification depends on the integrated effect of the shrinkage and the evolving elastic properties [39]. This simple picture does not account for stress relaxation and yielding. These effects are introduced briefly below and will be discussed further with stress measurement results in the subsequent sections.

Coatings are applied as viscous liquids and therefore develop viscous stress on deposition and the initial stages of shrinkage [54]. Assuming the viscous contribution to the stress is Newtonian, this contribution to stress is expressed as:

$$\sigma = \eta\dot{\varepsilon} \tag{2}$$

where η is the viscosity, which is a function of the amount of drying or curing, and $\dot{\varepsilon}$ is the strain rate or shrinkage rate. During the initial stages of drying or curing, the viscous contribution to stress dominates over the elastic, but the viscous stress is small (in comparison to the elastic stresses that develop after the coating solidifies) and is relaxed quickly. For viscoelastic materials, the polymer stress relaxation time scales with the ratio of viscosity to the shear modulus [1]. Early in the drying or curing process, the coating is still a liquid with a low viscosity and relaxation time is short [54]. However, as drying or curing proceeds, the coating structure changes and the viscosity climbs, resulting in longer and longer relaxation times. As the coating begins to support an elastic stress (i.e., solidifies), there is a competition between stress accumulation driven by the solidification (elastic) and stress relaxation (viscous), with the final state of stress depending on the time scales for the two processes and the evolving materials properties. In terms of the framework established above, relaxation involves a change in the stress-free state that reduces the strain (i.e., the difference between the current state and the stress-free state) and therefore the stress. See Fig. 1a.

As stress climbs, it can reach a level sufficient for plastic deformation or yielding. Ordinarily, plastic deformation is viewed as a permanent change in specimen dimensions. However, for a coating that is developing stress by drying or curing, the stress is not due to a macroscopic deformation, but rather the result of the departure of the coating's current state from its stress-free state [18, 50]. When a coating develops a stress equivalent to its yield stress, the stress-free state changes. For a perfectly plastic solid (no strain hardening), one would expect the difference between the stress-free state and the current state (the strain) to remain constant as shrinkage continues, resulting in a constant level of in-plane strain, and hence stress, as shrinkage proceeds. See Fig. 1b. For an elasto-viscoplastic material with a slow rate of post-yielding stress relaxation, the stress may climb beyond the yield stress and then relax over time back to the value of the yield stress, as described below. In a strain hardening material, the yield strength increases with further shrinkage and hence the stress in a strain hardening material continues to increase even after yielding.

Fig. 2 shows results from Lei's model for stress development in drying coatings [18, 50]. The model combines drying (i.e., diffusion and mass transfer) with a mechanical model for the coating that incorporates elastic deformation, yielding, and post-yielding viscous deformation (relaxation). The deformation is modeled based on the stress-free state, similar to Fig. 1. A total deformation gradient between the stress-free state and the current state is taken as the product of deformation gradients for three steps: shrinkage, viscoplastic yielding, and elastic deformation. Fig. 2a illustrates the differences between elastic, viscoelastic and elasto-viscoplastic behaviors. Stress climbs and levels off for the elastic case, develops and then decays back to zero for the viscoelastic, and climbs and relaxes back to a yield stress for the elasto-viscoplastic. Fig. 2b expands on the elasto-viscoplastic behavior showing the effect of post-yield stress relaxation. When stress relaxation is fast, increases in stress beyond the yield stress are quickly relaxed and the stress remains at the yield stress. When stress relaxation is slower, the stress in the coating surpasses the yield stress before relaxing back to a constant value. This example illustrates the complexities of interpreting stress measurement results.

3. Stress measurement techniques

The qualitative magnitude of stress in a coating can be surmised by observations. For coatings prepared on thin, low modulus substrates, coating stress is observed

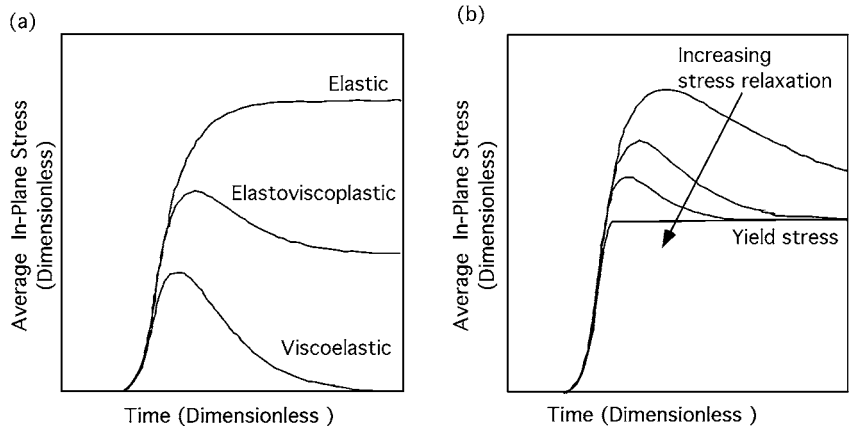

Figure 2 Schematic representation of results from an elasto-viscoplastic model for stress development during drying of a coating. (a) Comparison of elastic, elasto-viscoplastic and viscoelastic behavior. (b) Effect of stress relaxation after yielding. Adapted from Lei *et al*. [50].

as curling of the coated substrate. Curl may be compared on standard specimen geometries to determine the effects of process variables on stress [55]. However, quantifying the coating stress is difficult due to the extensive deformation of coating and substrate. Cracking is another defect that is indirectly linked to stress. The presence of cracks signals that a critical coating stress has been reached; however, this value of stress depends on the coating's thickness, fracture toughness and elastic properties [15, 16]. As in the case of curling, processing steps can be changed to eliminate cracking, but without further probing one cannot be sure if the changes have reduced stress or altered the mechanical properties of the coating, or both. The only practical solution to understanding stress and alleviating stress-induced defects is to quantify stress, and explore how processing variables affect stress and coating properties. To this end, measurements that allow stress to be monitored during processing are useful.

The most common method to determine coating stress is to measure the curvature or deflection of a coated elastic substrate (e.g., wafer or disk, strip, cantilever). This method dates back to 1909 with Stoney's work on electrodeposited coatings [56]. The basic assumptions and methodologies of curvature and deflection-based measurements of stress are outlined below, followed by a brief discussion of other stress measurement methods and supporting characterization methods. Complete descriptions of the mechanics involved in curvature and deflection-based techniques [4, 53, 57–61] and reviews of stress measurement methods [3, 7, 62] can be found in the literature.

The stress in a coating deforms the underlying substrate, resulting in a curvature of the system. See Fig. 3a. The coating stress (σ) can be determined from the radius of curvature (r), the coating thickness (t_c), the substrate thickness (t_s), the substrate elastic modulus (E_s), and the substrate Poisson's ratio (ν_s):

$$\sigma = \frac{E_s t_s^2}{(1-\nu_s)6rt_c} \tag{3}$$

This expression is derived assuming that the substrate and coating behave elastically with identical elastic moduli, the coating thickness is much less than the substrate thickness, and the coating is in a uniform state of biaxial stress. (The recognition that a biaxial stress state is more appropriate came after Stoney's original analysis [3].) By convention, tensile stress is positive and compressive negative. All of the parameters in Equation 3 can be measured easily. The substrate properties are determined by conventional mechanical tests. The

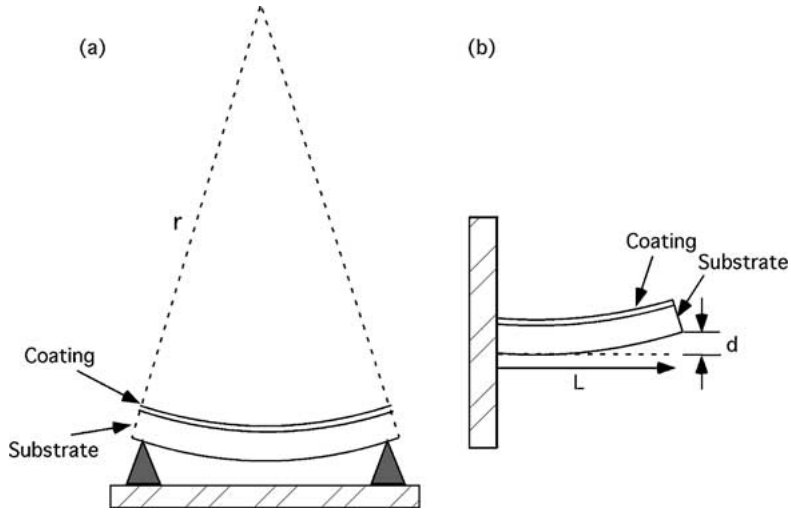

Figure 3 Set-ups for (a) curvature and (b) cantilever beam deflection methods for determining stress in coatings. Deformations are exaggerated. Adapted from Campbell [3].

coating thickness is easily measured at the end of drying and curing; however, when information about the evolution of stress is required, the final thickness is often used as an estimate of the coating thickness throughout. The radius of curvature can be monitored by scanning laser devices [5], profilometry, x-ray diffraction [63, 64] or interferometry [65]. Most importantly, one does not need to know the mechanical properties of the coating to determine its stress. Herein lies a great advantage of curvature and deflection-based measurements, because the mechanical properties of polymer coatings are difficult to quantify, especially as a function of drying or curing. Equation 3 neglects the fact that the stress in the coating is relieved due to the deformation of the substrate/coating pair. A correction factor may be added to account for this effect [5], but as will be noted below, experiments are typically designed so that curvature and hence the stress reduction by the curvature, is small enough to be ignored.

Instead of curvature, the displacement or deflection of a point(s) along the deformed substrate can be measured. A cantilever geometry is often chosen with the beam clamped on one end. See Fig. 3b. For this geometry, the radius of curvature is approximated by:

$$r = \frac{L^2}{2d} \tag{4}$$

where d is the deflection and L is the length from the clamp to where the deflection is measured; this expression assumes that $d \ll r$. Combining Equations 3 and 4 leads to a relationship between deflection and coating stress. Corcoran [59] considered a more general case, which accounts for the effect of bending on the coating stress:

$$\sigma = \frac{dE_s t_s^3}{3t_c L^2(t_s + t_c)(1 - \nu_s)} + \frac{dE_c(t_s + t_c)}{L^2(1 - \nu_c)} \tag{5}$$

where L is the distance from the clamp to the end of the cantilever (or the point at which deflection is measured), and the subscripts s and c refer to the substrate and coating, respectively. Assumptions made in deriving this equation include perfect adhesion between coating and substrate, no plastic deformation in substrate or coating, isotropic mechanical properties, a uniform state of biaxial stress in the coating, and small deflections relative to the substrate thickness. In Corcoran's derivation, the neutral axis is positioned midway through the substrate thickness, which is accurate when the substrate is much thicker and stiffer than the coating [60]. Equations similar to Equation 5 have been derived for more general beam bending problems in which the assumptions made by Corcoran do not necessarily hold [60, 62, 66].

The second term in Equation 5 accounts for the reduction in stress that occurs on bending. The error incurred by not including the second term increases as the coating thickness increases relative to the substrate thickness and as the coating modulus increases relative to the substrate modulus [59]. As an example consider stress measurement of a polymer coating on a steel cantilever ($E_s/E_c \sim 100$). Here, the ratio of the substrate thickness to the coating thickness should be at least ~5 to keep the error less than 1%. Ordinarily conditions are chosen ($E_s \gg E_c$ and $t_s \gg t_c$) so that the second term can be ignored and coating properties are not needed to determine the stress.

The deflection can be measured by a variety of methods, including optical microscopy, capacitance gauges, strain gauges and optical levers [3, 7, 62]. For accurate measurement of deflection it is important that the cantilever bends only along its length and not bend (or cup) appreciably in the width direction. To prevent cupping, the geometry of the cantilever must be chosen so that the length is much greater than the width. The necessary width-to-length ratio depends on the relative thicknesses and moduli of the substrate and coating [62]. Other considerations for cantilever beam-based measurements are discussed by Corcoran [59], and Perera and vanden Eynde [43].

Cantilever beam-based measurement systems lend themselves to the incorporation of special features. For example, Fig. 4 shows a system that combines coating application and processing with a cantilever beam-based stress measurement device [67]. The temperature and atmosphere of drying and curing are controlled, and special features such as a chilling chamber for gelatin coatings and a port for a UV source are incorporated [68]. The deflection is monitored continuously by an optical lever. This type of instrument has also been modified to include a video camera for simultaneous video monitoring of coating's optical characteristics during stress measurement and a balance for drying studies (carried out separately, but under identical conditions as stress measurement) [69, 70]. For simultaneous thickness measurement, similar devices have been equipped with an ellipsometer [71, 72] or a laser interferometer [73]. For curing studies, a cantilever-based device has been mounted in an FTIR to gain simultaneous curing and stress measurement data [74]. The beam bending method has also found application in the study of the interaction of polymer coatings with humid or solvent rich atmospheres, and water or other liquid environments [75–80].

While the cantilever method is widely used and has many advantages, its limitations should be noted. The stress measured by this method is an average stress. Stress gradients through the thickness of coating cannot be directly measured, though they may be surmised from thickness-dependent stress data [68, 81]. Equation 5 calls for the coating thickness, which varies as the coating dries or cures. Using of the final coating thickness to calculate stress throughout drying or curing leads to errors, especially in the early stages of stress development. Edge effects and thickness nonuniformities can also cloud the interpretation of the stress evolution data, depending on their severity. When the coating is mounted horizontally, as in Fig. 4, the changing weight of the coating contributes to the deflection and must be taken into account in the analysis. For coatings that solidify at high solids loadings, the correction is not typically carried out as the deflection due to weight loss is much less than that due to

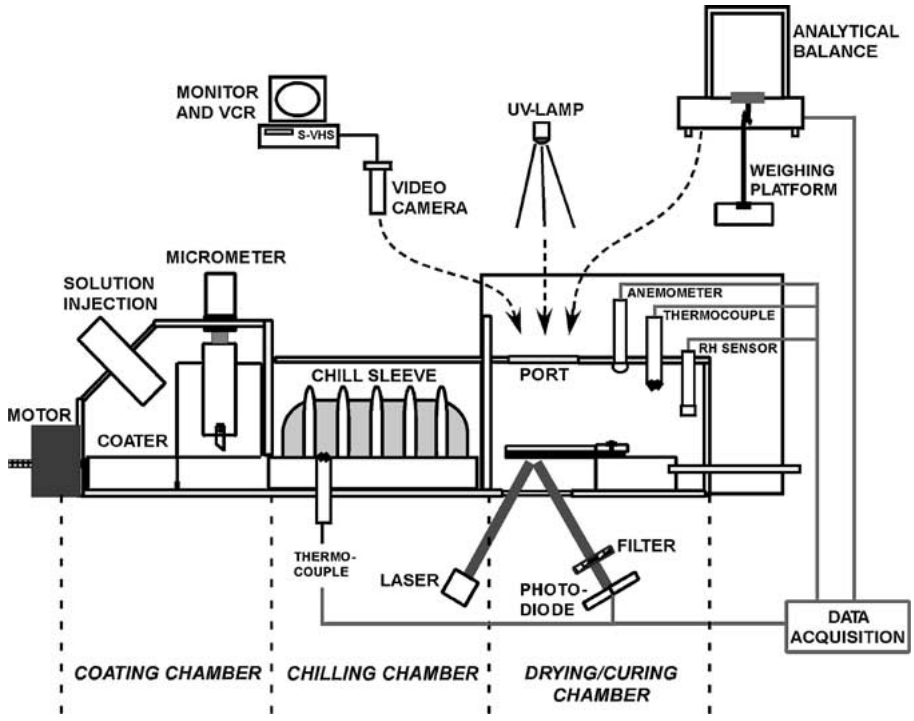

Figure 4 A stress measurement apparatus incorporating a draw-down coater, chiller, and drying/curing chamber with a cantilever beam deflection measurement device. Coating liquid is injected onto a beam, which is pulled beneath a blade, through a chilling chamber at low temperature (if desired) and then into the drying/curing chamber where deflection is measured as a function of time. Temperature and airflow are controlled in the final chamber. A port at the top of the chamber allows video monitoring of the coating, application of UV radiation or measurement of weight loss (in a separate experiment from deflection measurement). Adapted from [67–69].

coating stress development. Vertical mounting of the cantilever is possible; however, gravity-induced flow can be a limitation.

Curvature and deflection-based stress measurement systems can also be used to determine stress in multilayer coatings, though the interpretation of the data is more complex. Townsend and coworkers [82] developed a theory for elastic deformation in multilayer systems in which they show how each layer is independently responsible for a fraction of the curvature. Boerman and Perera [83] extended Corcoran's equation (Equation 5) to multilayer systems, and presented methods to determine the contributions of individual layers to the total stress. Similarly, Yan and White [84] and Bouchet and coworkers [85] analyzed the case of bilayer coatings.

There are other methods to measure stress in polymer coatings. Methods with spatial resolution bear special note. Stress-induced birefringence (photoelastic analysis) has been employed to show the stress distributions due to restrained shrinkage of polymer plates [86] and reveal stress in adhesive layers [87]. Shiga and coworkers [88] measured time resolved fluorescence from a label polymer added in small amounts to a coating. They used poly(3-octylthiophene), a conjugated polymer, as a fluorescent label. The fluorescence decay time was measured from coatings containing the label and compared to a calibration curve constructed using uniaxial tensile testing. Results were consistent with cantilever beam studies and since the technique targets a particular fluorescence, it can be used to resolve stress of a single coating in a multilayer stack. Another method with the promise of good spatial resolution is FTIR with a microscope attachment [89]. Stress is known to change the position, intensity or shape of some IR absorption bands. Like the fluorescence method, this technique requires calibration with tensile test results and is limited to certain polymers.

Interpretation of stress measurement data is facilitated by knowledge of the changing mechanical properties of coatings as they dry and cure. Much research has been devoted to characterization of the mechanical properties of coatings and thin films of all types and several reviews are in the literature on this topic [3, 4, 7, 46, 90–92]. Characterization of polymer coatings as they solidify is particularly difficult. Relatively few studies have quantified the elastic constants and yield strengths of polymers over a wide range of solvent contents [91, 93]. Likewise, quantification of the effect of the extent of cure on properties of UV or thermally curable polymer is also difficult [94]. One of the main challenges is to maintain a uniform solvent concentration or extent of cure throughout the test. Indentation methods hold promise for property measurement of polymer coatings [95, 96], perhaps even as they dry and cure. The field of mechanical properties of coatings and thin films has grown dramatically in recent years and offers promise for greater application to polymer coatings.

4. Stress development during drying

The stresses that originate during drying of thermoplastic polymer solution coatings have been investigated. Groundbreaking research took place in the 1970s and 1980s when Croll [31] and Perera [38, 39, 45] delved into the origins of stress and determined the effects of process variables on stress. More recently, researchers have been concerned with the stress development during the drying of other polymer coatings, including

coatings that gel and those prepared from multiple solvents. Latex-based coatings also develop stress on drying, and their stress development has been explored [40, 41, 70, 97]; however, these systems are beyond the scope of this paper. Likewise, thermal stresses can contribute to the final room temperature stress in polymer coatings, but here the emphasis is on isothermal studies. This section begins with a brief account of early research on drying of thermoplastic polymer coatings. An example of stress development during drying of a polymer coating is given to point out key features in the data. Lastly, results from some recent studies on stress development on drying are presented.

Croll [31–33] studied the stress in coatings prepared by casting a layer of polymer dissolved in a solvent and drying at room temperature. He proposed that the constrained shrinkage of the coating results in strain and that the strain depends on the solvent loss after solidification:

$$\varepsilon = \frac{\phi_s - \phi_r}{3(1 - \phi_r)} \tag{6}$$

where ϕ_s is the volume fraction of solvent at solidification and ϕ_r is the volume fraction of residual solvent. A key point, however, is defining solidification and estimating the solvent content at solidification. The glass transition temperature of a polymer/solvent system increases as the solvent departs. Croll defined solidification as the point at which the glass transition temperature reaches drying temperature. See Fig. 5. Stress values calculated using the calculated strains (Equation 6) and mechanical properties of the coatings after drying agreed fairly well with the stress determined from cantilever-based deflection measurements [32]. He found that the magnitude of the stress after drying is independent of the starting polymer concentration and the coating thickness for the systems he studied (polystyrene/toluene, polyisobutyl methacrylate/toluene). From these results, he concluded that stress was uniform through the thickness of the coating (or varied in the same way regardless of thickness) and that the longer times needed to dry the thicker coatings did not influence the final stress.

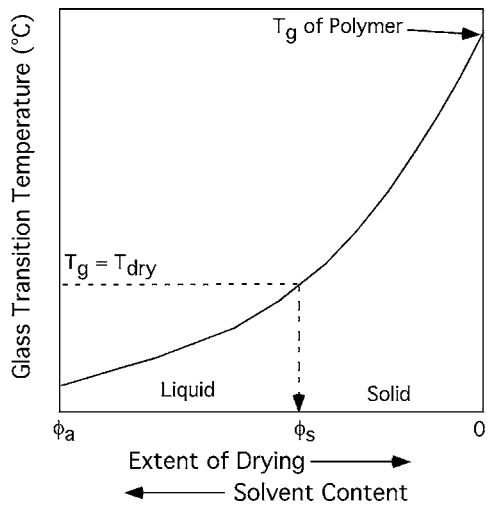

Figure 5 Effect of solvent content on glass transition temperature shown as a function of drying. The coating solution is prepared with a solvent content of ϕ_a and as it dries the solvent content decreases and the glass transition temperature increases. Solidification occurs when the solvent content has dropped to ϕ_s, where the glass transition temperature is equal to the drying temperature (T_{dry}). Adapted from Croll [31, 32].

The effects of several materials and processing variables can be understood in the context of Croll's model. For a given drying temperature, polymers with lower glass transition temperatures (T_g) will tend to solidify with less solvent trapped and hence experience less constrained shrinkage after solidification. Moran and Whitmore [98] show this trend for poly(vinyl acetates) and poly(methacrylates). Plasticizers lower T_g, which results in less solvent trapped at solidification and less strain from constrained shrinkage. For a given amount of strain, stress values will be lower for polymers with lower elastic moduli (see Equation 1). Hence, stresses decrease with decreasing polymer T_g (or increasing plasticizer content) due to the lower moduli in addition to the lower amounts of constrained shrinkage. In fact, Croll [32] reported a higher final stress for polystyrene ($T_g = 100°C$) coatings compared with polyisobutyl methacrylate ($T_g = 58°C$) coatings, each cast from a solution in toluene. While the strains calculated from Equation 6 were not much different between these two, polystyrene had a higher stress due, in large part, to its higher modulus. Lastly, drying at a higher temperature leads to a lower stress due to the lower solvent content at solidification and therefore less constrained shrinkage after solidification. However, thermal stresses may also contribute to the overall stress at room temperature, depending on the thermal expansion mismatch between coating and substrate.

The evolution of stress during drying is also important to understanding the origin of stress. Fig. 6 shows stress measurement and drying data for a coating prepared from a solution of cellulose acetate in acetone [69]. Cellulose acetate is a glassy polymer with a T_g of 185°C. The drying data are typical of a polymer/solvent coating [13, 99–101]. Weight loss is rapid initially. The supply of solvent at the coating surface is nearly constant and drying is limited by external conditions, such as air flow. Little stress develops in the early stages of drying because the coating has not yet solidified; its modulus is low and stress relaxation is relatively fast. With further drying, the coating solidifies and the measured stress climbs as more solvent is lost

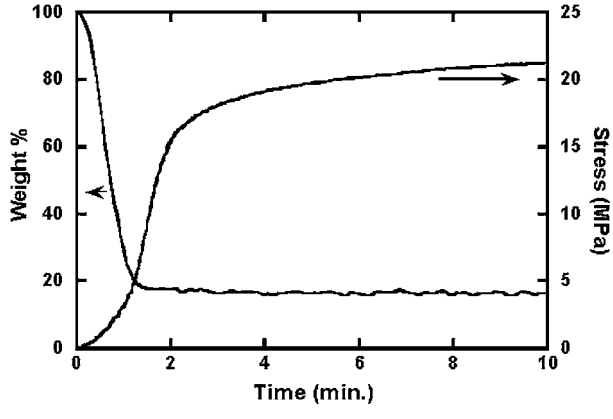

Figure 6 Stress development and drying data for a coating prepared from a cellulose acetate solution (10 wt%) in acetone. Stress development and drying were recorded on separate coatings prepared under identical conditions. Adapted from Vaessen *et al.* [69].

(strain increases). In addition, the modulus of the coating grows. The drying rate falls as the solvent becomes depleted and the process becomes limited by diffusion of solvent through the coating. Even after the drying rate has fallen off significantly, stress continues to accumulate in this coating, because even a tiny amount of shrinkage leads to a strain. Due to the relatively high modulus of the coating at the end of drying, the small strain results in a noticeable increase in stress.

Solvent type influences the stress development of a drying polymer coating. Perera and vanden Eynde [39] showed that the use of solvents that dry more slowly results in coatings with lower final stresses. The properties of a coating change during the course of drying, which Perera and vanden Eynde [39] account for using a drying time dependent elastic modulus and Poisson's ratio in Equation 1. By examining drying and stress data, they conclude the coating modulus is kept lower over the course of solidification for the slower drying solvents and more stress relaxation can occur, leading to a lower stress at the end of drying. Whitmore *et al.* [30] also showed the same trend in their work with coatings for art preservation.

Working with mixed solvent systems can also lead to interesting microstructures and stress development features. The drying coatings discussed thus far have consisted of a uniform structure with no microstructural features. In the field of polymer membranes, porous coatings are made by drying a polymer solution that contains a poorer, slower evaporating non-solvent along with a good, faster evaporating solvent [102, 103]. On drying, the composition is forced into a two-phase region of the ternary phase diagram and a polymer-rich and a polymer-lean phase develop. With further drying, the polymer-rich phase vitrifies and the volatiles in the polymer-lean phase evaporate to form pores. In Fig. 7, the development of stress in these phase separating coatings is compared with similar coatings that do not phase separate [69]. The evolution is affected by the pore formation. Stress climbs as usual, but then drops likely due to the release of a small amount of capillary stress as the liquid menisci descend into the pores. In addition, porous coatings develop a lower final stress; pore formation requires there to be less shrinkage (strain) compared with a dense coating and pores also lower the coating modulus. Also interesting are coatings prepared from solutions containing more non-solvent initially (not shown); these coatings form larger pores in addition to the small pores and have an additional feature, a plateau, early in the stress development data. The plateau in the stress appears to indicate that the larger pores form by a stress-induced rupture process. Prakash [104] first proposed this mechanism based on cryo-scanning electron microscopy studies.

Complex microstructures and interesting stress development on drying can also be found in studies of stress in tape-cast ceramic layers [105, 106]. Tape-cast coatings are prepared from a dispersion of ceramic particles in a liquid containing a polymer binder and a plasticizer, which is coated and dried. Typically, the volume ratio of ceramic to binder is on the order of 2:1. After drying, the composite coating is removed from the substrate and fired to make a ceramic sheet. Lewis and coworkers [105–107] have shown that the stress development in these composites systems is dictated in part by the stress development in the polymeric binder phase. Fig. 8 compares the stress development in the polymer binder phase with that from the tape-cast coating containing ceramic [105]. Like the polymer

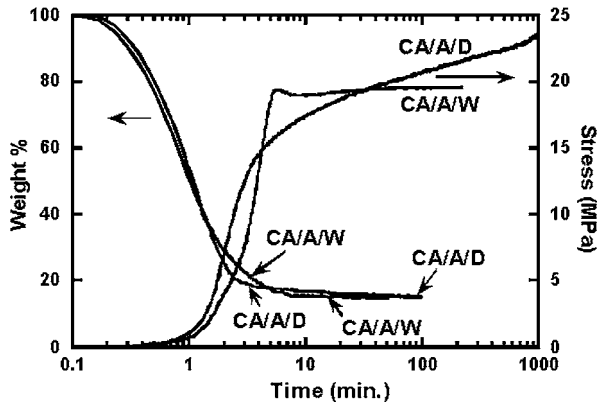

Figure 7 Stress development and weight loss data for: CA/A/D coatings prepared from a 10 wt% cellulose acetate solution in acetone (80 wt%) and dioxane (10 wt%) and CA/A/W coating prepared from a 10 wt% cellulose acetate coating in acetone (80 wt%) and water (10 wt%). Water and dioxane have similar volatilities, but water is a nonsolvent for cellulose acetate and dioxane is a solvent. Note that time is given on a log scale. Adapted from Vaessen *et al.* [69].

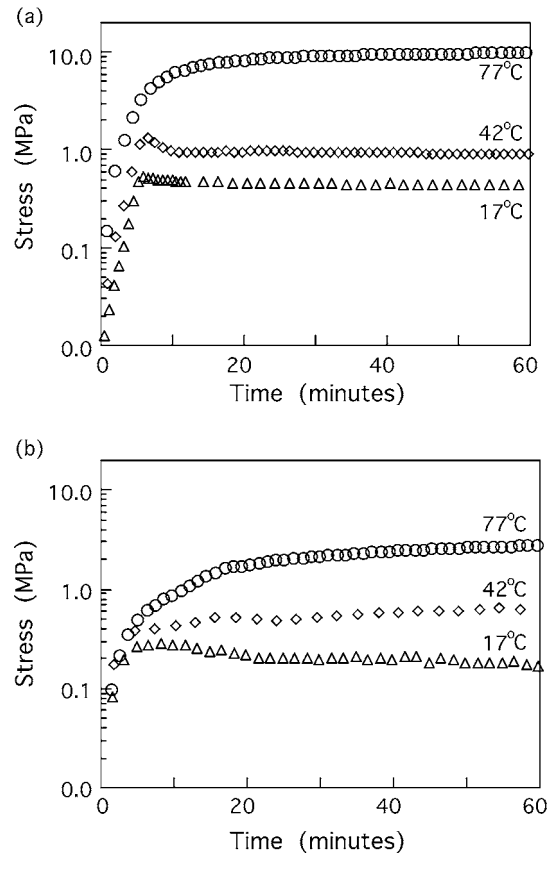

Figure 8 (a) Stress development during drying coatings from suspensions containing Al_2O_3 particles (20 vol%) in a suspension with poly(vinyl butyral) (PVB) and dibutyl phthalate (DBP) plasticizer in methyl ethyl ketone: tolulene (1 : 1 by wt). The ratio of PVB:DBP was varied so that the binder glass transition temperature (T_g) varied from 17 to 77°C, as labeled. (b) Stress development during drying of PVB/DBP binder solution coatings of various T_g values as labeled. Note stress is shown on a log scale. Adapted from Payne [62] and Lewis *et al.* [105].

systems alone, tapes prepared with plasticizer have a lower stress and therefore have the advantage of greater dimensional stability after their removal from the substrate. More complex polymer binding phases that gel (or crosslink) are needed in gel-casting of ceramics; here too, drying-induced stresses have been measured [107]. Changes in the polymer, in this case poly(vinyl alcohol), led to variations in the stress development in the composite layers. Crosslinking of the polymer phase led to a decrease in stress relaxation after drying, resulting in higher overall stress.

Stress development studies on drying of aqueous gelatin coatings demonstrate the effects of processing variables on stress development [71, 108]. In the processing of gelatin layers in photographic film, an aqueous solution of gelatin is cast and then chilled to form gel via physical crosslinks and then dried. One might expect stress to be influenced by the gelation step, in addition to the drying conditions. However, Payne and coworkers [108], using the apparatus pictured in Fig. 4, showed that the chilling step itself did not have much of an effect on the final stress in the gelatin coating. The drying conditions, including temperature and relative humidity, affect the stress development significantly. See Fig. 9. Increasing the temperature of drying led to lower stresses, due to the lower amount of solvent loss after solidification, decreased elastic modulus and increased stress relaxation. With increasing relative humidity, the stress is lower. The high relative humidity slowed drying, providing more opportunity for stress relaxation, and resulted in less constrained shrinkage.

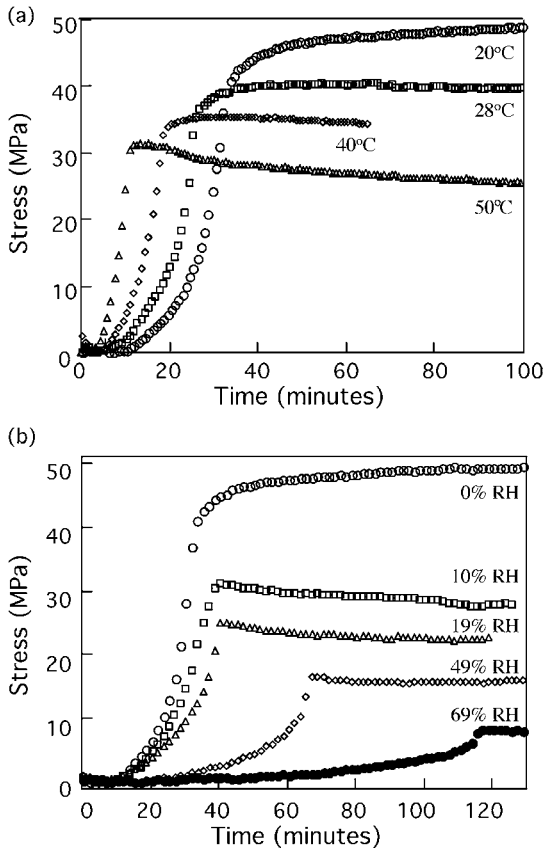

Figure 9 Stress development during drying of gelatin coatings: (a) effect of drying temperature at 0% relative humidity and (b) effect of relative humidity during drying. Adapted from Payne *et al*. [108].

In addition, the modulus of gelatin is lower and stress relaxation faster with the greater water content. By cycling the relative humidity in the atmosphere, the stress responds by increasing under low relative humidity and decreasing under high relative humidity [71, 108]. Hysteresis is observed, however, indicating a permanent change in the stress-free state or yielding. The experimental data [108] agree with theoretical predictions for an elasto-viscoplastic coating [50].

5. Stress development during curing

Understanding and predicting stress in curing coatings is as important as it is in drying coatings. Shrinkage due to reaction can be 20% or more in some curing polymer systems [109]. While only the shrinkage after solidification results in stress, stresses in the tens of MPa are not uncommon in coatings prepared by curing. Thus, delamination, cracking, crazing, and wrinkling problems are frequently encountered. Many processing variables influence the development of structure and stress in curing coatings; however, there have been few systematic studies of stress development in these materials. Moreover, in thermally curing coatings not all stress studies are conducted isothermally, so in such cases it is necessary to distinguish between stresses originating from curing and those originating from thermal expansion mismatch as the system is heated and cooled through a curing cycle.

This section reviews the most systematic studies of stress in curing coatings to-date, focusing on stress arising from isothermal reaction rather than from temperature changes. Systems that have been given the most thorough attention to-date are epoxy thermal curing (through condensation polymerization) and acrylate (or methacrylate) photo-induced curing (through addition polymerization). Since most of the attention in curing systems has focused on crosslinking polymerization (particularly epoxy-amine and multifunctional acrylates and methacrylates), purely linearly polymerizing coatings will not be considered. Further, we will confine our attention to solvent-free, porogen-free, and filler-free curing polymer systems (e.g., necessarily excluding porous low-K dielectric films, polyimides and dental curing systems). In this paper, the term "curing coatings" is meant to entail these conditions. Although there is considerable interest in non-uniform cure through the thickness (e.g., for control of surface finish, for deliberate skinning, etc.), we have found no systematic study of stress development in such coatings. Therefore, the focus here is on those systems that have been cured uniformly through the entire thickness of the coating.

The stages in stress development in curing coatings have analogies to those in drying systems; reaction proceeds until the coating solidifies, and beyond this point stress develops because of the frustration of in-plane shrinkage that accompanies reaction. Fig. 10 [62, 68] shows typical features in the conversion and stress profiles exhibited by an isothermal curing system—in this case, a UV-cured multifunctional acrylate coating. Note that some reaction proceeds before the coating solidifies and stress begins to register. After solidification,

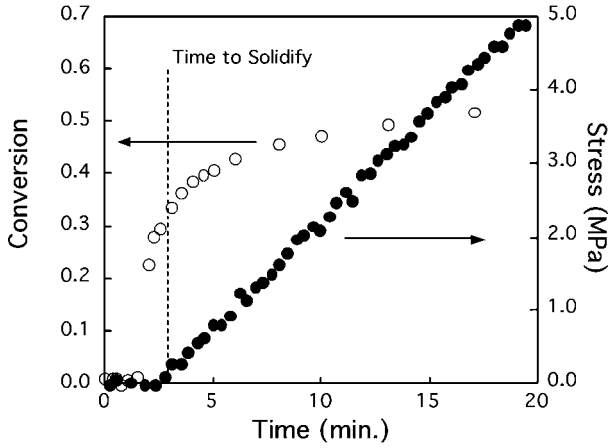

Figure 10 Stress development and conversion data for a UV cured acrylate coating (trimethylol propane triacrylate with 0.5 wt% 2,2-dimethoxy-2-phenylacetophenone, DMPA, photoinitiator). Stress and conversion data were taken separately, but under identical conditions. The coating was cured with an intensity of 2.1 W/m^2 using UV source with a peak wavelength of 365 nm. Adapted from Payne *et al*. [68].

stress continues to climb with further reaction and constrained shrinkage.

Several clarifications to this simple analogy, though, are required when considering solidification by reaction. First, of course, instead of decreasing solvent fraction it is increasing conversion that leads to solidification. That is, as the conversion increases, the glass transition temperature of the reacting mixture increases eventually reaching room temperature. This behavior is similar to that shown in Fig. 5, but with the x-axis as the extent of cure and instead of a solvent content at solidification (or a vitrification solvent content), there is a vitrification conversion.

Second, before the conversion reaches a vitrification conversion, gelation might occur [110–113]. In other words, the reactions may set up a network polymer gel (still swollen by its parent monomer) well before this polymer becomes densely crosslinked enough to vitrify [109, 114]. However, the work discussed below suggests that the modulus and relaxation times of such gels are low enough that not very much stress develops in the gelled state before vitrification. Fig. 11 illustrates the salient differences between the weak gel solid and the stronger vitreous solid state. In most cases it is assumed, and we will see that experiment tends to confirm, that vitrification, with its vastly larger increase in modulus, dominates stress development. (Moreover, Zumbrum *et al.* [114] provide a very clear demonstration that it is vitrification, not gelation, that dominates the dramatic slowing of cure in acrylate systems.) However, because the amount and rate of shrinkage while in the gel state could conceivably be high, significant stress might develop in the gelled state. Moreover, gelation may play a significant role in the stress development in coatings that both dry and cure. Though not within the scope of this section, such coatings (for instance, sol-gel coatings) might develop significant stress in the gel state because of the removal of a vast amount of solvent in the gel state, entailing (among other things) a huge amount of potential shrinkage, capillary forces as menisci enter the porespace, and further curing reactions with the collapse of pores.

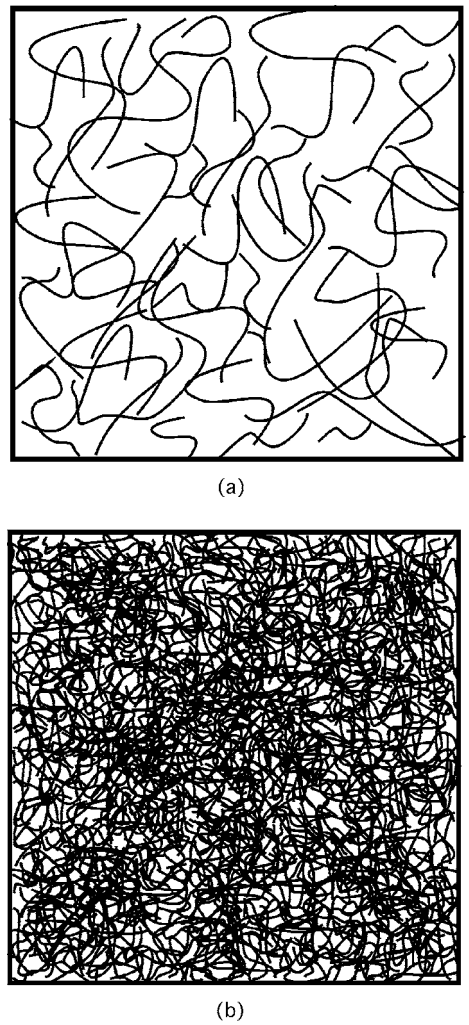

Figure 11 Conceptual diagram of a gelled state (a) as compared with a (b) vitrified state (light regions are filled with unreacted monomer.) Though the gelled state should exhibit an elastic modulus, that modulus will be low and relaxation through segmental motion should be facile. In contrast, the vitrified state should show a high modulus and slow relaxation.

The third feature of curing coatings that deserves special note is that it is very common for curing coatings to be left with incomplete conversion; curing reactions slow significantly once the coating has vitrified. Coating practitioners are not as likely to directly measure residual functional group concentration (and to try to eliminate it) as they are to measure and try to eliminate residual solvent content in drying coatings.

Fourth, it is thought that in at least some systems an accelerated curing rate can increase the achievable conversion, perhaps because shrinkage due to the reaction does not have time to occur and so excess free volume remains, enabling reactive groups to remain mobile to higher conversions [115–118].

Fifth, there is an enormous range of composition, crosslink density, and detailed polymer structure that is opened up when one begins to consider building the polymer from monomers and oligomers *in situ*. Sixth, kinetic models for this structural development are often less certain than drying rate models, particularly when microgelation and other non-idealities and diffusion restrictions occur (even though curing takes place uniformly through the thickness of the film). Finally, models to predict the conversion needed to form a gel

or glass (gelation conversion and vitrification conversion, respectively) are less well-established than those to predict solvent content at which the glass transition temperature is equal to the drying temperature for coatings that solidify by drying.

Croll [34] was one of the first to quantify stress development in curing epoxy coatings. He noted the danger that stress in these coatings might be influenced by absorption of moisture (leading to an unexpected thickness dependence). He also established that one can readily ensure that, even though the curing reaction is exothermic, the coating temperature can be made uniform with industrially relevant coating thicknesses, curing rates and heat transfer coefficients.

More recently, Lange and coworkers [119–121] measured the stress in epoxy coatings with some variety of formulations (acrylates were also studied; these are addressed below). Much of the work was non-isothermal, but they took care to report on what portion of the stress appeared to have been generated exclusively by reaction. When the coating is cured at a temperature that is above the ultimate glass transition temperature, very little stress is generated (though there can be substantial thermal mismatch stress upon cooling below T_g). When the coating is cured below the ultimate T_g, a significant amount of stress can be generated when dense crosslinking is allowed (up to 2 MPa with an average functionality of 4.5, though the actual crosslink density achieved was not reported), but a lightly crosslinking formulation (average functionality 2) gave less than 0.1 MPa curing stress (though thermal stress was still significant). The authors noted that gelation could be detected distinct from vitrification in rheological tests, but it did not appear that significant stress was generated (cf. the order of 1 MPa) in the gelled state—significant stress appeared only after vitrification.

Further work by Lange and coworkers [122–124] has also been done to better understand the nature of gelation and vitrification, the mechanical properties, and heterogeneities, such as hyperbranched polymers or microgels forming during the epoxy cure. Though these trends have not yet been used to predict or better understand stress development explicitly, these researchers point out in earlier papers [119–121] how one can predict the stress using elastic analysis from the experimentally measured elastic modulus and shrinkage (in thickness) (or, alternatively, with viscoelastic stress analysis from the experimentally measured elastic and relaxation modulus and shrinkage).

Other work that has focused on predicting the elastic and relaxation moduli and/or shrinkage in epoxy coatings includes that of Gillham and coworkers [110–113] (to be discussed further below), Adolf and coworkers [125, 126], Chambers *et al.* [127], and Plazek and Chay [128]. There has also been a fair amount of work refining the curing kinetic models to better incorporate diffusional constraints as the polymer network crosslinks (e.g., Matsuoka *et al.* [129]). These groups of contributions use different modeling assumptions (sometimes assuming the availability of certain experimental data such as modulus as a function of conversion or sometimes assuming certain functional forms with parameters to be fit to experiment), and they do not all attempt to predict the same collection of properties. However, these models offer a great deal of hope that it will become possible to quantitatively predict, model, and perhaps design and control curing stress.

For instance, Gillham and coworkers [110–113] have been able to predict "time-temperature-transformation" diagrams and "continuous heating transformation" diagrams for epoxy coatings. These are operating diagrams, validated experimentally, that predict the gelation and vitrification times, and the evolution of T_g with time, for various curing protocols. It does not appear that this approach has yet been extended to predict stress, but there is every indication that such an extension is possible.

Though somewhat beyond the scope of this review, it is worthwhile to note an additional contribution in the epoxy field beyond coatings. Madhukar and coworkers [130] have pointed out that it is important to limit the degree of cure in epoxy/fiber composites to avoid excessive cure-induced stress that can weaken the fiber/matrix composite. We will see in the following that an analogous caution should be kept in mind when curing coatings as well.

Isothermal curing to high crosslink density coatings, at very convenient temperatures, is routinely accomplished by the radiation-induced addition polymerization of multifunctional acrylates and methacrylates [131–133]. The radiation may be electron beams or, more commonly, ultraviolet (UV) light (with photoinitiators added to the coating solution). UV curing is growing in use because one can quickly cure to glassy, tough, impermeable coatings at low temperature with no emission of volatiles. High functionality monomers are increasingly used to solidify the coating at lower light doses (allowing lower photoinitiator concentration, weaker light sources, and/or faster line speeds), to increase the apparent ultimate glass transition temperature, and to make stronger and more impermeable coatings. However, these measures can also aggravate the problems of unreacted acrylate groups, incomplete use of photoinitiators and trapped free radicals—all of which can lead to undesired, further reaction well after the deliberate curing is over. The effects of processing variables—photoinitiator concentration, light intensity and wavelength, and coating formulation—on conversion have been reported, but there was little systematic work showing stress development in acrylates systems until the 1990s. Since bulk free-body shrinkage can range from 10 to 30% by volume, Blanding *et al.* [109] noted early on that significant coating stress should be expected when curing coatings of multifunctional acrylates.

Lange and coworkers [120, 121, 134] showed for several acrylate coatings (as they did for epoxy coatings discussed above) that increasing the crosslink density tends to increase stress. They found that acrylates show higher stress than epoxy coatings when monomers are selected to give comparable expected crosslink densities (though actual crosslink densities were not measured). Particularly when the acrylate is cured at a temperature above the ultimate T_g, the stress contribution from curing was shown to be as high as 39 MPa—an

order of magnitude higher than that developed by a comparable epoxy coating.

Payne *et al.* [68] reported a study of stress development and conversion development in the isothermal, room temperature UV-curing of triacrylate and tetraacrylate coatings. They found that significant stress developed only when the conversion reached about half of its final value (see Fig. 10), and that, beyond a point, continued irradiation causes a great deal of stress with very little extra conversion. Moreover, they found more stress in the tetraacrylate system, even though its conversion was only about three-fourths that of the triacrylate (thus establishing a comparable crosslink density). In addition to the monomer functionality, they systematically examined the effects of photoinitiator concentration, light intensity, and coating thickness. They reported that the stress grew more rapidly, to higher magnitudes (up to 30 MPa) with more photoinitiator or stronger light, and they suggested further attention to the roles that plasticizers and post-cure temperature cycles could play in relaxing stress. Beyond the scope of this review, they also reported conditions leading to nonuniform cure.

This contribution raised two important questions: (1) whether accelerating cure to increase conversion also significantly increases stress, and (2) whether the dependence of stress on conversion should depend on cure rate. Wen *et al.* [52] examined a variety of systems, comparable to Payne *et al.* [68], and provided answers to these questions. They applied Croll's hypothesis that stress development scales with volume shrinkage after solidification to these curing systems and found it to be correct in all but the fastest curing systems examined. In all cases, significant (cf. 1 MPa) stress did not develop until relatively high conversions were achieved—conversions far too high to correspond to gelation, but rather which must correspond to vitrification. (Wen [52] even suggested the measurement of stress as a plausible method to detect the isothermal vitrification conversion.) The vitrification conversion fell when conditions favored more rigid networks (higher monomer functionality, shorter monomer chain length, lower plasticizer concentration, and the use of methacrylate groups). After the vitrification conversion, stress was roughly proportional to the excess conversion, the proportionality being higher with the growth of more rigid networks, as illustrated in Fig. 12.

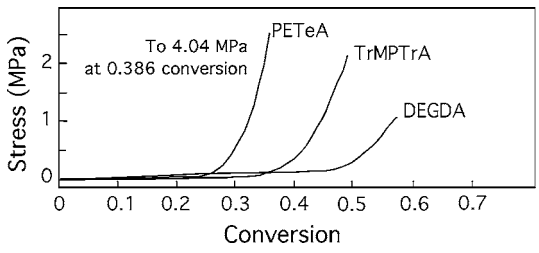

Figure 12 Stress development as a function of conversion for different diacrylate monomers: pentaerythritol tetraacrylate (PETeA), trimethylopropane trimethacrylate (TrMPTra) and diethylene glycol diacrylate (DEGDA). 2,2-dimethoxy-2-phenylacetophenone, DMPA, photoinitiator was used at a 1 wt% level in each coating and curing was carried out with an intensity of 40 W/m^2 using UV source with a peak wavelength of 365 nm. Adapted from Wen *et al.* [52].

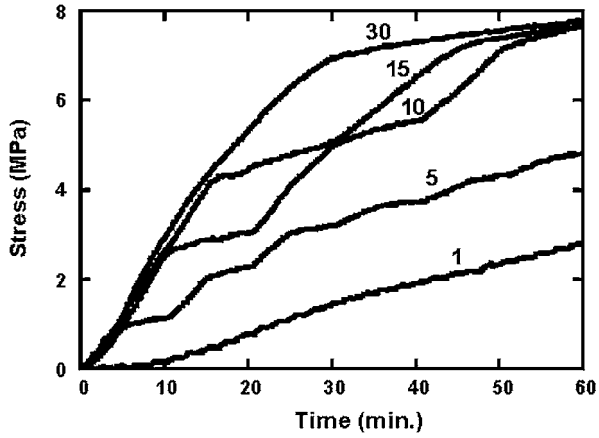

Figure 13 Effect of cycling the UV source on stress development for an acrylate coating (trimethylol propane triacrylate with 1.3 wt% 2,2-dimethoxy-2-phenylacetophenone, DMPA, photoinitiator). Coating was cured with an intensity of 1 W/m^2 using UV source with a peak wavelength of 365 nm. Curves are labeled with half-cycle times (in minutes), each coating was exposed to the same total dose. Adapted from Vaessen *et al.* [135].

Wen found that accelerating the rate of cure by increasing the light intensity also led to an increase in stress; however, lowering the functionality, adding plasticizer and other means could be employed to increase conversion rate without increasing stress.

Vaessen *et al.* [135] considered the question whether deliberately placed dark periods might allow polymerization to slow (or, if radicals terminate or trap readily enough, actually stop) for periods and so allow internal segment motion to cause relaxation of stress. To promote stress relaxation during the cure of a triacrylate coating, they cycled the power to the UV lamp, examining the effect of the cycle period while keeping the total dose constant. They found that one could choose the cycle period so as to reduce the final stress at least 60% while accomplishing essentially identical conversion and mechanical properties. See Fig. 13. They suggested that the optimal curing schedule might be designed by introducing dark periods that correspond to characteristic relaxation times of network segments.

Another common strategy to reduce stress is to attempt to relax stress at high temperatures. We have taken care to restrict our attention, to the degree possible, to isothermal studies, but one should take note of two reports of perhaps counterintuitive results. Cook [136] notes that increasing the temperature during the UV cure can actually decrease the conversion achieved—presumably by accelerating termination more than propagation. Moreover, Blanding *et al.* [109] note that in some coatings attempts to "anneal" the coating after cure actually increases stress—presumably by liberating trapped radicals, enabling further curing, or by volume relaxation (physical aging).

In most of the UV curing stress work to-date, conversion and stress have been measured separately under conditions as close to identical as could be achieved. Progress on this front has been reported, though, with a device capable of simultaneous conversion and stress measurement [74, 137]. The results show that the development of conversion and stress with curing time

follows trends suggested previously by separate measurements of conversion and stress [68].

The experimental work to-date on UV curing coatings exposes the potential profit of models (such as those developed for epoxies) to predict cure kinetics, network relaxation times, vitrification, and modulus. This pursuit seems to be more challenging for multifunctional acrylates than for epoxies. There has been significant progress on this front, though several complications appear that are characteristic of addition polymerization in crosslinking systems. In a body of work starting in the mid-1980s, Boots, Kloosterboer and coworkers [115–118, 138] and Peppas, Bowman, Anseth, and coworkers [139–148] have ably demonstrated that the kinetics of such systems are to be understood only with insight into how the structure of the network is built. Multifunctional acrylates can crosslink so readily that even at very low conversions tightly cyclized and crosslinked microgels can form. The apparent gelation and vitrification of these polymer systems must be understood as the filling of space with such heterogeneous structures. Only recently is it becoming clear how such complex structure development might influence the modulus, relaxation times, and stress development in these coatings. Fortunately, though, more experimental measurements are being reported so that the crosslinking structure and mechanical properties more predictable (e.g., [94, 115, 118, 149–153]). There is considerable interest to predict a radiation curing formulation and protocol that can lead to a high crosslinking conversion with low stress.

Despite the extensive use of polyester, polyurethane, and other curing systems in protective, adhesive, and functional coatings, we have found no body of work comparable to the epoxy and acrylate studies above in the measurement and prediction of stress development. There is a pronounced need not only for experimental measurements of stress development, but more importantly for such measurements that are systematically performed to enable formulation and testing of models.

6. Final remarks

Measurements of stress development in polymer coatings have led to a greater understanding of the origin of stress and have led to strategies for decreasing stress and the incidence of stress-induced defects. While the evolution of a coating from an as-applied liquid to a final solid is complex, the relatively simple principle that stress is the consequence of the strain due to constrained shrinkage after solidification has proven a solid paradigm for both drying and curing coatings. On this foundation, continued research will result in a better understanding and control of stress in the future. In particular, measurements of the changing rheological and mechanical properties of coatings as they dry and cure are needed. Among other purposes, these measurements serve as inputs to models for stress development. New or improved stress measurement methods that allow spatial resolution will be important as tools to understand and better control stress-related defects as well as the complex stresses in multilayer structures. Lastly, stress measurements of the type featured in this paper are needed as new coatings, particularly those with complex chemistries and microstructures, are introduced.

Acknowledgements

The authors acknowledge support from the Center for Interfacial Engineering, an NSF sponsored Engineering Research Center at the University of Minnesota through its Coating Process Fundamentals Program, the industrial sponsors of the Coating Process Fundamentals Program, and DuPont through a young professor grant. JAP and DMV also acknowledge the Graduate School at the University of Minnesota for Doctoral Dissertation Fellowships. The authors also thank Dr. S-Y. Tam, Dr. H. Lei, Dr. M. Wen, V. Rajamani, Professor H. K. Stolarski, Professor W. W. Gerberich, Professor R. F. Cook and especially Professor L. E. Scriven for insight into the development of stresses in polymer coatings.

References

1. L. H. SPERLING, "Introduction to Physical Polymer Science" (John Wiley, New York, 1992).
2. C. A. FLEISCHER, C. L. BAUER, E. J. MASSA and J. F. TAYLOR, *MRS Bulletin* **21** (1996) 14.
3. D. S. CAMPBELL, in "Handbook of Thin Film Technology," edited by L. I. Maissel and R. Glang (McGraw-Hill, New York, 1969) p. 12.
4. R. W. HOFFMAN, in "Physics of Non-Metallic Thin Films," edited by C. H. S. Dupuy and A. Chachard (Plenum, New York, 1976) p. 273.
5. P. A. FLINN, D. S. GARDNER and W. D. NIX, *IEEE Trans. Electron Devices* **34** (1987) 689.
6. M. F. DOERNER and W. D. NIX, in "CRC Critical Reviews in Solid State and Materials Sciences" (CRC Publishing, 1988) p. 225.
7. M. OHRING, "The Materials Science of Thin Films" (Academic Press, New York, 1992).
8. T. KOUFOPOULOS and P. S. THEOCARIS, *J. Composite Materials* **3** (1969) 308.
9. S. R. WHITE and H. T. HAHN, *ibid.* **26** (1992) 2423.
10. S. MOTAHHARI and J. CAMERON, *J. Reinforced Plastics and Composites* **18** (1999) 1011.
11. E. D. COHEN and E. J. LIGHTFOOT, *Chem. Eng. Prog.* (1990) 30.
12. C. H. HARE, *J. Protective Coating and Linings* **13** (1996) 99.
13. E. D. COHEN, in "Modern Coating and Drying Technology," edited by E. D. Cohen and E. B. Gutoff (VCH Publishers, New York, 1992) p. 267.
14. K. SATO, *Prog. Org. Coatings* **8** (1980) 143.
15. A. G. EVANS, M. D. DRORY and M. S. HU, *J. Mater. Res.* **3** (1988) 1043.
16. M. D. THOULESS, *J. Vac. Sci. Technol.* A **9** (1991) 2510.
17. H. LEI, L. F. FRANCIS, W. W. GERBERICH and L. E. SCRIVEN, in "Multiscale Modeling of Materials," edited by L. P. Kubin, J. L. Bassanni, K. Cho and R. L. B. Selinger, MRS Proceedings Vol. 653 (Materials Research Society, Pittsburgh, PA, 2000). p. Z10.5.
18. H. LEI. Ph.D. thesis, University of Minnesota, 1999.
19. K. N. CHRISTODOULOU, E. J. LIGHTFOOT and R. W. POWELL, *AIChE J.* **44** (1998) 1484.
20. S. G. CROLL, *J. Coatings Tech.* **52** (1980) 35.
21. R. W. HOFFMAN, *Surface and Interface Analysis* **3** (1981) 62.
22. M. D. THOULESS, *Acta Metall.* **36** (1988) 3131.
23. H. LEI, L. F. FRANCIS, W. W. GERBERICH and L. E. SCRIVEN, *AIChE J.* **48** (2002) 437.
24. E. SUHIR, *Polym. Eng. Sci.* **30** (1990) 108.
25. H.-K. CHANG and Y.-K. KIM, *Sensors and Actuators* A: *Physical* **84** (2000) 342.
26. E. B. GUTOFF and E. D. COHEN, "Coating and Drying Defects: Troubleshooting Operating Problems" (J. Wiley and Sons, New York, 1995).

27. R. A. DICKIE, *Prog. Org. Coatings* **25** (1994) 3.
28. T.-J. CHUANG, T. NGUYEN and S. LEE, *J. Coatings Tech.* **71** (1999) 75.
29. D. Y. PERERA, in "Plastics and Coatings Durability, Stabilization, Testing," edited by R. A. Ryntz (Hanser Gardner Publications, Cincinnati, OH, 2001) p. 115.
30. P. M. WHITMORE, D. MORAN and C. BAILIE, *JAIC* **38** (1999) 429.
31. S. G. CROLL, *J. Coatings Tech.* **50** (1978) 33.
32. *Idem.*, *J. Appl. Polym. Sci.* **23** (1979) 847.
33. *Idem.*, *J. Coatings Tech.* **51** (1979) 64.
34. *Idem.*, *ibid.* **51** (1979) 49.
35. *Idem.*, *Polymer* **20** (1979) 1423.
36. *Idem.*, *J. Coatings Tech.* **53** (1981) 85.
37. *Idem.*, *Adhesion Aspects Polym.* (1981) 107.
38. D. Y. PERERA and D. VANDEN EYNDE, *J. Coatings Tech.* **53** (1981) 40.
39. *Idem.*, *ibid.* **55** (1983) 37.
40. D. Y. PERERA, *ibid.* **56** (1984) 111.
41. D. Y. PERERA and D. VANDEN EYNDE, *ibid.* **56** (1984) 47.
42. *Idem.*, *ibid.* **56** (1984) 69.
43. *Idem.*, *ibid.* **53** (1984) 39.
44. *Idem.*, *ibid.* **59** (1987) 55.
45. M. OOSTERBROEK, R. J. LAMMERS, L. G. J. VAN DER VEN and D. Y. PERERA, *ibid.* **63** (1991) 55.
46. R. W. HOFFMAN, in "Physics of Thin Films," Vol. 3. edited by G. Hass and R. E. Thun (McGraw Hill, New York, 1966) 211.
47. L. E. SCRIVEN, "Coating Process Fundamentals Short Course" (University of Minnesota, 1996).
48. S. Y. TAM, L. E. SCRIVEN and H. K. STOLARSKI, in "Thin Films—Stresses and Mechanical Properties V," edited by S. P. Baker, P. Borgesen, P. H. Townsend, C. A. Ross and C. A. Volkert, MRS Proceedings Vol. 356 (Materials Research Society, Pittsburgh, PA, 1995) p. 547.
49. S.-Y. TAM, Ph.D. thesis, University of Minnesota, 1997.
50. H. LEI, J. A. PAYNE, A. V. McCORMICK, L. F. FRANCIS, W. W. GERBERICH and L. E. SCRIVEN, *J. Appl. Polym. Sci.* **81** (2001) 1000.
51. M. WEN, Ph.D. thesis, University of Minnesota, 2001.
52. M. WEN, L. E. SCRIVEN and A. V. McCORMICK, *Macromolecules* **35** (2002) 112.
53. Y. INOUE and Y. KOBATAKE, *Appl. Sci. Res.* A **7** (1958) 314.
54. R. R. MYERS, *J. Polym Sci.: Polym. Symp.* **35** (1971) 3.
55. J. Q. UMBERGER, *Photographic Science and Engineering* **1** (1957) 69.
56. G. G. STONEY, *Proc. Royal Soc. London* Series A **82** (1909) 172.
57. S. P TIMOSHENKO, *J. Opt. Soc. Am.* **11** (1925) 233.
58. A. BRENNER and S. SENDEROFF, *J. Res. Nat. Bur. Stand.* **42** (1949) 105.
59. E. M. CORCORAN, *J. Paint Technology* **41** (1969) 635.
60. C.-C. CHIU, *J. Amer. Ceram. Soc.* **73** (1990) 1999.
61. M. BENABDI and A. A. ROCHE, *J. Adhesion Sci. Technol.* **11** (1997) 281.
62. J. A. PAYNE, Ph.D. thesis, University of Minnesota, 1998.
63. C. GOLDSMITH, *J. Vacuum Sci. Tech.* A **1** (1983) 407.
64. L. T. NGUYEN, in "New Characterization Techniques for Thin Polymer Films," edited by H.-M. Tong and L. T. Nguyen (John Wiley & Sons, New York, 1990) p. 57.
65. R. C. CHIU and M. J. CIMA, *J. Amer. Ceram. Soc.* **76** (1993) 2769.
66. M. BENABDI and A. A. ROCHE, *J. Adhesion Sci. Technol.* **11** (1997) 373.
67. J. A. PAYNE, A. V. McCORMICK and L. F. FRANCIS, *Rev. Sci. Instrum.* **68** (1997) 4564.
68. J. A. PAYNE, L. F. FRANCIS and A. V. McCORMICK, *J. Appl. Polym. Sci.* **66** (1997) 1267.
69. D. M. VAESSEN, A. V. McCORMICK and L. F. FRANCIS, *Polymer* **43** (2002) 2267.
70. C. J. MARTINEZ and J. A. LEWIS, *Langmuir* **18** (2002) 4689.
71. M. LU, S.-Y. TAM, P. R. SCHUNK and C. J. BRINKER, in "Thin Films—Stresses and Mechanical Properties VIII," edited by R. Vinci, O. Kraft, N. Moody, P. Besser and E. Schaffer II (Materials Research Society, Pittsburgh, PA, 2000) p. 263.
72. M. LU and C. J. BRINKER, in "Thin Films—Stresses and Mechanical Properties VIII," edited by R. Vinci, O. Kraft, N. Moody, P. Besser and E. Schaffer II (Materials Research Society, Pittsburgh, PA, 2000) p. 463.
73. K. S. PARK, Y. D. KWON and D. KIM, *Polym. J.* **33** (2001) 503.
74. A. A. STOLOV, T. XIE, J. PENELLE and S. HSU, *Macromolecules* **33** (2000) 6970.
75. B. S. BERRY and W. C. PRITCHET, *IBM J. Res. Develop.* **28** (1984) 662.
76. H.-M. TONG and K. L. SAENGER, in "New Characterization Techniques for Thin Polymer Films," edited by H-M. Tong and N. T. Nguyen (John Wiley & Sons, New York, 1990) p. 29.
77. J. H. JOU, L. HSU, P. T. HUANG, R. HUANG and W. P. SHEN, *Polymer J.* **23** (1991) 1123.
78. D. Y. PERERA and D. VANDEN EYNDE, *J. Coatings Tech.* **59** (1987) 55.
79. G. YAN and J. R. WHITE, *Poly. Eng. Sci.* **39** (1999) 1866.
80. D. F. STAMATIALIS, M. SANOPOIPOU and I. RAPTIS, *J. Appl. Poly. Sci.* **83** (2002) 2823.
81. S. G. CROLL, *J. Coating Tech.* **52** (1980) 65.
82. P. H. TOWNSEND, D. M. BARNETT and T. A. BRUNNER, *J. Appl. Phys.* **62** (1987) 4438.
83. A. E. BOERMAN and D. Y. PERERA, *J. Coating Tech.* **70** (1998) 69.
84. G. YAN and J. R. WHITE, *Polym. Sci. and Eng.* **39** (1999) 1856.
85. J. BOUCHET, A. A. ROCHE and E. JACQUELIN, *J. Adhesion Sci. Tech.* **15** (2001) 321.
86. V. J. PARKS and A. J. DURELLI, *J. Appl. Mechanics* **32** (1965) 504.
87. Y. NIITSU, K. ICHINOSE and K. IKEGAMI, *JSME International J.* A **38** (1995) 68.
88. T. SHIGA, T. NARITA, K. TACHI, A. OKADA, H. TAKAHASHI and T. KURAUCHI, *Poly. Eng. Sci.* **37** (1997) 24.
89. O. LOURIE, H. D. WAGNER and N. LEVIN, *Polymer* **38** (1997) 5699.
90. A. ZOSEL, *Prog. Org. Coatings* **8** (1980) 47.
91. C. J. KNAUSS, in "Surface Coatings," edited by A. D. Wilson, J. W. Nicholson and H. J. Prosser (Elsevier Applied Science, London, 1987) p. 232.
92. F. R. BRONTZEN, *International Materials Reviews* **39** (1994) 24.
93. K. S. RAJU and R. R. MYERS, *J. Coatings Tech.* **53** (1981) 31.
94. S. S. LEE, A. LUCIANI and J.-A. MANSON, *Prog. Org. Coatings* **38** (2000) 193.
95. A. STROJNY, X. XIA, A. TSOU and W. W. GERBERICH, *J. Adhes. Sci. Tech.* **12** (1998) 1299.
96. M. DABRAL, X. XIA, W. W. GERBERICH, L. F. FRANCIS and L. E. SCRIVEN, *J. Polym. Sci. B Polym. Physics* **39** (2001) 1824.
97. C. PETERSEN, C. HELDMANN and D. JOHANNSMANN, *Langmuir* **15** (1999) 7745.
98. D. MORAN and P. M. WHITMORE, in "Materials Issues in Art and Archaeology IV," edited by J. R. D. P. B. Vandiver, J. M. G. Madrid, I. C. Freestone and G. S. Wheeler (Materials Research Society, Pittsburgh, PA, 1995) p. 293.
99. R. A. CAIRNCROSS, L. F. FRANCIS and L. E. SCRIVEN, *Drying Technology* **10** (1992) 893.
100. J. S. VRENTAS and C. M. VRENTAS, *J. Polym Sci B: Polym. Phys.* **32** (1994) 187.
101. S. ALSOY and J. L. DUDA, *Drying Technology* **16** (1998) 15.
102. M. MULDER, "Basic Principles of Membrane Technology" (Kluwer Academic, Dordrecht, The Netherlands, 1991).
103. L. ZEMAN and T. FRASER, *J. Membrane Sci.* **74** (1993) 93.
104. S. S. PRAKASH, Ph.D. thesis, University of Minnesota, 2001.
105. J. A. LEWIS, K. A. BLACKMAN, A. L. OGDEN, J. A. PAYNE and L. F. FRANCIS, *J. Amer. Ceram. Soc.* **79** (1996) 3225.
106. J. E. SMAY and J. A. LEWIS, *ibid.* **84** (2001) 2495.
107. M. HUHA and J. A. LEWIS, *ibid.* **83** (2000) 1957.

108. J. A. PAYNE, A. V. McCORMICK and L. F. FRANCIS, *J. Appl. Polym. Sci.* **73** (1999) 553.
109. J. M. BLANDING, C. L. OSBORN and S. L. WATSON, *J. Radiation Curing* **13** (1978).
110. M. T. ARONHIME and J. K. GILLHAM, *J. Coatings Tech.* **56** (1984) 35.
111. J. B. ENNS and J. K. GILLHAM, *J. Appl. Polym. Sci.* **28** (1983) 2567.
112. S. L. SIMON and J. K. GILLHAM, *J. Coatings Tech.* **95** (1993) 57.
113. X. WANG and J. K. GILLHAM, *J. Appl. Poly. Sci.* **47** (1993) 425.
114. M. A. ZUMBRUM, G. L. WILKES and T. C. WARD, in "Radiation Curing in Polymer Science and Technology," edited by J.-P. Fourassier and J. F. Rabek (Elsevier, London, 1993) p. 101.
115. J. G. KLOOSTERBOER, R. G. VAN DE HEI and H. M. J. BOOTS, *Polym. Comm.* **25** (1984) 355.
116. H. M. BOOTS, J. G. KLOOSTERBOER, G. M. M. VANDEHEI and R. B. PANDEY, *Brit. Polym. J.* **17** (1985) 219.
117. J. G. KLOOSTERBOER, G. M. M. VAN DE HEI, R. G. GOSSINK and G. C. M. DORTANT, *Polym. Comm.* **25** (1984) 322.
118. J. G. KLOOSTERBOER and G. F. C. M. LIJTEN, *Polymer* **31** (1990) 95.
119. J. LANGE, S. TOLL, J. E. MANSON and A. HULT, *ibid.* **36** (1995) 3135.
120. J. LANGE, J. E. MANSON and A. HULT, *ibid.* **37** (1996) 5859.
121. J. LANGE, S. TOLL, J. E. MANSON and A. HULT, *ibid.* **38** (1997) 809.
122. J. LANGE, *Poly, Eng. Sci.* **39** (1999) 1651.
123. J. LANGE, M. JOHANSSON, C. T. KELLY and P. J. HALLEY, *Polymer* **40** (1999) 5699.
124. J. LANGE, R. EKELOF and G. A. GEORGE, *ibid.* **40** (1999) 3595.
125. D. ADOLF and J. E. MARTIN, *Macromolecules* **23** (1990) 3700.
126. D. B. ADOLF and R. S. CHAMBERS, *Polymer* **38** (1997) 5481.
127. R. S. CHAMBERS, R. R. LAGASSE, T. R. GUESS, D. J. PLAZEK and C. BERO, *J. Electronic Packaging* **117** (1995) 249.
128. D. J. PLAZEK and I.-C. CHAY, *J. Polym. Sci B: Polymer. Phys. Ed.* **29** (1991) 17.
129. S. MATSUOKA, X. QUAN, H. E. BAIR and D. J. BOYLE, *Macromolecules* **22** (1989) 4093.
130. J. D. RUSSEL, M. S. MADHUKAR, M. S. GENIDY and A. Y. LEE, *J. Composite Materials* **34** (2000) 1926.
131. C. DECKER, *Polym. Internat.* **45** (1998) 133.
132. S. P. PAPPAS, "Radiation Curing: Science and Technology," edited by S. P. Pappas (Plenum, New York, 1992).
133. C. G. ROFFEY, "Photopolymerization of Surface Coatings" (J. Wiley and Sons, Chichester, 1982).
134. J. LANGE and J. E. MANSON, *Polymer* **37** (1996) 5859.
135. D. M. VAESSEN, F. A. NGANTUNG, M. B. PALICIO, L. F. FRANCIS and A. V. McCORMICK, *J. Appl. Poly. Sci.* **84** (2002) 2784.
136. W. D. COOK, *Polymer* **33** (1992) 2152.
137. A. STOLOV, T. XIE, J. PENELLE and S. L. HSU, *Polym. Mater. Sci. Eng.* **82** (2000) 371.
138. H. M. BOOTS and R. B. PANDEY, *Polym. Bull.* **11** (1984) 415.
139. K. S. ANSETH, C. N. BOWMAN and N. A. PEPPAS, *J. Polym. Sci A: Polymer. Chem. Ed.* **32** (1994) 139.
140. K. S. ANSETH, C. M. WANG and C. N. BOWMAN, *Polymer* **35** (1994) 3243.
141. *Idem.*, *Macromolecules* **27** (1994) 650.
142. K. S. ANSETH and C. N. BOWMAN, *Chem. Eng. Sci.* **49** (1994) 2207.
143. K. S. ANSETH, L. M. KLINE, T. A. WALDER, K. ANDERSON and C. N. BOWMAN, *Macromolecules* **28** (1995) 2491.
144. K. S. ANSETH, K. J. ANDERSON and C. N. BOWMAN, *Macromol. Chem. Phys.* **197** (1996) 833.
145. M. H. BLAND and N. A. PEPPAS, *Biomaterials* **17** (1996) 1109.
146. C. N. BOWMAN and N. A. PEPPAS, *Macromolecules* **24** (1991) 1914.
147. *Idem.*, *J. Polym. Sci. Part A Polymer Chem. Ed.* **29** (1991) 1575.
148. *Idem.*, *Chem. Eng. Sci.* **47** (1992) 1411.
149. J. BICERANO, R. L. SAMMLER, C. J. CARRIERE and J. T. SIETZ, *J. Polym. Sci B: Polymer Phys. Ed.* **34** (1996) 2247.
150. J. E. DIETZ and N. A. PEPPAS, *Polymer* **38** (1997) 3767.
151. M. D. GOODNER, H. R. LEE and C. N. BOWMAN, *Ind. Eng. Chem. Res.* **35** (1997) 1247.
152. A. R. KANNURPATTI, K. S. ANSETH and C. N. BOWMAN, *Polymer* **39** (1998) 2507.
153. D. L. KURDIKAR and N. A. PEPPAS, *Macromolecules* **27** (1994) 4084.

Received 10 April
and accepted 7 June 2002